NeuroImage: Clinical 22 (2019) 101782

Contents lists available at ScienceDirect

NeuroImage: Clinical

journal homepage: www.elsevier.com/locate/ynicl

Resting state connectivity best predicts alcohol use severity in moderate to heavy alcohol users

Samantha J. Fede[a], Erica N. Grodin[a,1], Sarah F. Dean[a], Nancy Diazgranados[b], Reza Momenan[a,*]

[a] Clinical NeuroImaging Research Core, National Institute of Alcohol Abuse and Alcoholism, National Institutes of Health, 10 Center Drive, Bethesda, MD 20814, MSC 1108, United States

[b] Office of Clinical Director, National Institute of Alcohol Abuse and Alcoholism, National Institutes of Health, 10 Center Drive, Bethesda, MD 20814, MSC 1108, United States

ARTICLE INFO

Keywords:
Alcohol use disorder
MRI
Machine learning
Multimodal
Connectivity
Imaging

ABSTRACT

Background: In the United States, 13% of adults are estimated to have alcohol use disorder (AUD). Most studies examining the neurobiology of AUD treat individuals with this disorder as a homogeneous group; however, the theories of the neurocircuitry of AUD call for a quantitative and dimensional approach. Previous imaging studies find differences in brain structure, function, and resting-state connectivity in AUD, but few use a multimodal approach to understand the association between severity of alcohol use and the brain differences.

Methods: Adults (ages 22–60) with problem drinking patterns (n = 59) completed a behavioral and neuroimaging protocol at the National Institutes of Health. Alcohol severity was quantified with the Alcohol Use Disorders Identification Test (AUDIT). In a 3 T MRI scanner, participants underwent a structural MRI as well as resting-state, monetary incentive delay, and face matching fMRI scans. Machine learning was applied and trained using the neural data from MRI scanning. The model was tested for generalizability in a validation sample (n = 24).

Results: The resting state-connectivity features model best predicted AUD severity in the naïve sample, compared to task fMRI, structural MRI, combined MRI features, or demographic features. Network connectivity features between salience network, default mode network, executive control network, and sensory networks explained 33% of the variance associated with AUDIT in this model.

Conclusions: These findings indicate that the neural effects of AUD vary according to severity. Our results emphasize the utility of resting state fMRI as a neuroimaging biomarker for quantitative clinical evaluation of AUD.

1. Introduction

Alcohol use is highly prevalent in the United States, with 56% of adults reporting drinking in the past month (SAMHSA, 2015). Nearly half of those individuals also report problem alcohol use patterns, such that 23% of alcohol drinkers are estimated to have alcohol use disorder (AUD). More than just common, alcohol misuse is estimated to cost $249 billion every year in the United states and account for nearly 100,000 deaths yearly (Sacks et al., 2015).

Currently, less than 10% of people affected by AUD receive treatment, and research findings on medications and therapy are inconsistent or small in effect (Kranzler and Kirk, 2001; Miller and Wilbourne, 2002; SAMHSA, 2015). Part of the struggle to reduce alcohol misuse and its negative impacts is a lack of understanding of AUD across the spectrum of severity, which may require different approaches to treatment (Epstein et al., 2002; Moss et al., 2007). Most studies examine the neurobiology of AUD through dichotomous analysis of patients versus controls (Beck et al., 2009; Heinz et al., 2004). It is especially necessary to understand AUD as a dimensional condition given its complex underpinnings. A prominent theory of AUD includes three interconnected neurocircuits that underlie the cycle of addiction: binge/intoxication (reward and reinforcement processes in the basal ganglia networks); withdrawal/negative affect (engaging salience network regions in the extended amygdala and portions of the nucleus accumbens); and preoccupation/ anticipation “craving” (salience network with connections to default mode and executive control networks in conditioned incentive salience processes; Koob and Volkow, 2016). One explanation of the mechanism underlying this cycle is that chronic alcohol use is associated with a reduction in mesolimbic dopaminergic neurocircuitry followed by compensatory recruitment of systems associated with stress response (Vengeliene et al., 2008). However, these reviews and others (e.g., Sullivan and Pfefferbaum, 2005) suggest that

* Corresponding author.
E-mail addresses: fedesj@nih.gov (S.J. Fede), rezam@nih.gov (R. Momenan).
[1] Currently affiliated with Addictions Lab, Psychology, University of California, Los Angeles, United States.

https://doi.org/10.1016/j.nicl.2019.101782
Received 18 October 2018; Received in revised form 7 February 2019; Accepted 14 March 2019
Available online 19 March 2019

alcohol use impacts a wide variety of brain networks.

There is substantial research on neural differences during task-based fMRI associated with AUD. According to a meta-analysis, alcohol cues elicit greater neural engagement in individuals with AUD compared to controls in the default mode network (DMN; e.g., posterior cingulate (PCC)/ precuneus, and superior temporal gyrus), salience network (SN; e.g., the ventral striatum (VS)), and executive control network regions (ECN; e.g., anterior cingulate (ACC), and medial prefrontal cortex (mPFC); Myrick et al., 2004). Individuals with AUD may also have differential neural activity associated with impulse control (Li et al., 2009), response to emotional cues (Gilman and Hommer, 2008), response inhibition (Ames et al., 2014), and risk-taking (Claus and Hutchison, 2012). More severe AUD is related to engagement of SN/ basal ganglia network structures during alcohol taste cued craving (Filbey et al., 2008), impulsive choice (E. D. Claus et al., 2011a), and selection of alcoholic versus non-alcoholic beverages (Stuke et al., 2016).

The effects of short- and long-term alcohol use on resting state functional magnetic resonance imaging (rs-fMRI) dynamics have been previously examined. AUD individuals have increased between network but weaker within network connectivity than controls, particularly within ECN, DMN, basal ganglia, SN, and visual networks (Chanraud et al., 2011; Muller-Oehring et al., 2015; Weiland et al., 2014; Zhu et al., 2017; Zhu et al., 2018; Zilverstand et al., 2018). An study of dynamic network connectivity during rest suggests reduced occupancy of states characterized by salience-motor-sensory network connectivity (Vergara et al., 2018). As individuals with AUD are abstinent, rs-fMRI synchrony progressively decreases within reward networks but increases in executive control networks (Camchong et al., 2013b). Acute alcohol intoxication moderates functional connectivity during rs-fMRI (Khalili-Mahani et al., 2012), and is associated with increased visual network and frontal theta engagement (Esposito et al., 2010; Lei et al., 2014; Spagnolli et al., 2013). Atypical neural dynamics during rs-fMRI may be a pre-existing risk factor for AUD (Cservenka et al., 2014). Importantly for treatment, some findings suggest that rs-fMRI antisynchrony can also be used as a success marker for treatment (Schmaal et al., 2013) and synchrony as a risk factor for relapse (Camchong et al., 2013a).

There are also demonstrated associations between AUD and gray matter volume (GMV). In individuals with AUD, lifetime duration of alcohol use is negatively associated with GMV in the whole brain (Fein et al., 2002). In another study, individuals with AUD had less GMV than healthy subjects in ECN (dorsolateral prefrontal cortex (dlPFC), mPFC/ ACC) and DMN regions (parietal-occipital) region, predicting relapse (Rando et al., 2011). Other studies suggest these GMV deficits associated with AUD may be even more extensive, including differences in SN subcortical volumes (Grodin et al., 2013; Yang et al., 2016).

Alzheimer's and mild cognitive impairment have been studied extensively using multimodal approaches, finding that structural, functional, and cerebrospinal fluid measures in combination best predict outcomes (Vemuri et al., 2009; Yassa et al., 2010; Zhang et al., 2011). Some work suggests that together rs-fMRI and task-fMRI paradigms contribute to understanding the neural basis of disorders, such as schizophrenia, and behavior, like sense of self and response time (Du et al., 2012; Kelly et al., 2008; Qin and Northoff, 2011). Multimodal imaging may also be useful in predicting outcomes like substance use treatment completion and rearrest (Fink et al., 2016; Steele et al., 2015). Overall, these approaches may contribute distinct utility for use in patient groups. However, in the AUD field, few studies quantitatively compare or combine rs-fMRI, task-fMRI, and structural MRI (sMRI), particularly in terms of clinical utility. Vergara and colleagues demonstrate some shared variation and unique contributions between genetic, sMRI, and rs-fMRI data in binge-drinking individuals; however, this study does not investigate the relationship between this correspondence and AUD severity (Vergara et al., 2014). Squeglia and colleagues conducted a random forest analysis finding thinner cortices and less brain activity during cognitive control contributed to predicting alcohol initation in adolescence (Squeglia et al., 2017); however, they did not report overall model accuracy nor looked at a generalization sample.

In this study, we aimed 1) to use functional network connectivity derived from rs-fMRI, fMRI during tasks of emotional face processing and monetary incentive delay, and GMV to predict alcohol use severity, as measured by the Alcohol Use Disorders Identification Test (AUDIT). We also aimed 2) to compare the predictive utility of rs-fMRI, task-fMRI, and sMRI findings. We hypothesized that neural features corresponding to the salience network, default mode network, executive control network, and basal ganglia network would predict AUD severity. We also expected that the combined features would perform better than any set of features on their own. Although previous studies from our group have used machine learning to classify individuals as AUD or control based on rs-fMRI with 87% accuracy (Zhu et al., 2018), the current study is the first to use machine learning to predict AUD severity based on combined rs-fMRI, task-fMRI, and sMRI features.

2. Methods and materials

2.1. Participants

2.1.1. Primary sample

Adult men and women with moderate to heavy alcohol use ($N = 59$) completed a neuroimaging protocol at the National Institutes of Alcohol Abuse and Alcoholism (NIAAA). Participants were recruited from NIAAA inpatient treatment and from the community (See Supplemental Table 3 for the demographic features of inpatient and outpatient samples). This study was carried out in accordance with and as approved by the National Institutes of Health Addictions Institutional Review Board. All participants gave written, informed consent in accordance with the Declaration of Helsinki. See Table 1(A & C) for a description of the sample demographics. Exclusion criteria were as follows: currently experiencing withdrawal from alcohol, left handedness, currently testing positive for drugs (THC, cocaine, methamphetamine, opiates, or benzodiazepine), or MRI contraindicated. Additionally, participants with IQ < 70 or age > 60 were excluded from analysis. The final sample included four subjects with one comorbid substance use disorder (cannabis abuse, mild cannabis use disorder, cocaine abuse, and anxiolytic dependence). This sub-group (75% male, 50% inpatient) did not differ significantly from the overall sample on age, IQ, years of education, AUDIT, average drinks per day, or Fagerstrom Test of Nicotine Dependence smoking score (Heatherton et al., 1991).

2.1.2. Validation sample

Participants ($n = 24$) were recruited and included based on the procedures described above. See Table 1(B & D) for a description of sample demographics.

2.2. Behavioral data collection

Participants completed a standardized screening procedure, including demographic, health, and alcohol use information. We collected the AUDIT to measure problem alcohol use severity; when we refer to alcohol use severity, we are referring to score on the AUDIT, rather than DSM-5 diagnosed disorder severity. The AUDIT is a 10-item self-report measure covering alcohol consumption, drinking behavior, and alcohol-related problems (Saunders et al., 1993). Each item is scored between 0 (least severe) and 4 (most severe). When the AUDIT is used for diagnosis, a score of 8 or above is suggested to indicate AUD (Conigrave et al., 1995a). Average number of consumed alcoholic drinks per day was collected using the Alcohol Timeline Follow Back, which assesses drinking over the last 90 days (Sobell and Sobell, 2000). We also collected the Wechsler Abbreviated Scale of Intelligence II (WASI) to assess IQ (Wechsler, 2011). The WASI is a short form

Table 1
Sample demographics.

A.	Primary sample				B.	Validation sample			
	Mean	STDev	Min	Max		Mean	STDev	Min	Max
AUDIT	24.25	8.46	7	38		26.14	7.88	7	38
Age	41.14	11.00	22	60		41.25	11.14	25	60
IQ	99.75	15.98	73	144		105.79	16.88	74	141
Education	13.97	2.51	7	20		14.29	2.48	10	19
Drinks/day	13.06	9.57	1.69	42		11.57	8.03	1.56	36.67
Fagerstrom	1.78	2.53	0	9		1.17	2.02	0	7
Gender		male: 67.80%					male: 50.00%		
Treatment Status		inpatient: 67.80%					inpatient: 79.17%		
Smoking Status		smoker: 40.35%					smoker: 39.13%		

C.	Age	Education	IQ	Drinks/Day	Fagerstrom	D.	Age	Education	IQ	Drinks/Day	Fagerstrom
Education	−0.11						−0.19				
IQ	-0.25^{+}	0.33*					−0.21	0.67***			
Drinks/day	0.01	−0.17	−0.14				0.33	-0.38^{+}	−0.59**		
Fagerstrom	0.14	−0.05	−0.11	−0.20			0.15	-0.37^{+}	−0.06	0.33	
AUDIT	0.23^{+}	−0.19	0.17	0.56**	0.10		−0.13	−0.28	−0.24	0.55**	0.27

Notes: (A) Primary sample descriptive statistics and frequencies. (B) Validation sample descriptives and frequencies. (C) Correlations between measures within the primary sample. (D) Correlations between measures within the validation sample. Significance as follows: $^{+}$: $p < .1$. *$p < .05$, **$p < .001$. There were no significant differences between the primary and validation samples on demographic variables.

measurement to estimate intelligence based on two-subtests: vocabulary and matrix reasoning. The Fagerstrom Test for Nicotine Dependence was collected to quantify levels of smoking (Heatherton et al., 1991). Participants were breathalyzed at the beginning of each study visit, and were not run with a blood alcohol level > 0.00 g/dl.

2.3. fMRI tasks

2.3.1. Monetary Incentive Delay (MID) Task

Anticipation of monetary reward and loss was measured following a modified version of the procedures described in Knutson et al., 2001. During this task, participants saw cue symbols to indicate one of five conditions: 1) *low reward* (win $0.20), 2) *high reward* (win $1.00), 3) *low loss* (lose $0.20), 4) *high loss* (lose $1.00), and 5) *neutral* (no loss or reward). Following this cue at a variable interval (2000–2500 msec), the participant responded to a target stimulus with a button press. For reward conditions, successfully pressing during the target period resulted in receipt of monetary reward. For loss conditions, failing to press during the target period resulted in loss of monetary reward. Failure to hit a reward target, successfully hitting a loss target, and all responses to neutral targets did not result in any monetary outcome. Participants were given feedback after another jittered delay of 1500–5000 msec following their button press. There were 17 trials per cue type.

2.3.2. Face matching task

Processing of emotional faces was measured following a modified version of the procedures described in Hariri et al., 2002. During this task, participants viewed a target picture and two additional pictures; participants were instructed to select the picture that matched the target by pressing the corresponding button. Six types of pictures were shown: 1) angry faces, 2) sad faces, 3) fearful faces, 4) happy faces, 5) neutral faces, and 6) shapes. There were two interleaved blocks of each picture type. Prior to each block, instructions were presented for two seconds for subjects to “match shapes” or “match faces”. Each block contained 6 images of the same type, displayed for 5 s with no inter-stimulus interval, for a total of 30 s per block. Male and female faces were equally represented. For the purpose of this study, we focused on negative emotional faces because the previous literature has consistently found alcohol-related effects in this domain (Charlet et al., 2014; Salloum et al., 2007) and in fact have used happy faces as a control condition in some cases (Sripada et al., 2011). This task is an implicit processing task; behavioral responses were not of interest and thus not included in the model.

2.4. Imaging data acquisition

Participants were scanned on a Siemens 3T Skyra Magnetic Resonance Imaging (MRI) machine at the NIH Clinical Center. While in the scanner, they completed a sMRI scan, a rs-fMRI scan, and then two task- fMRI scans, described above. For the rs-fMRI, participants lay in the dark for ten minutes with eyes open and no additional stimuli. All three functional scans were acquired using an echoplanar-imaging pulse sequence (TR: 2000 msec, TE: 30 msec, flip angle: 90°, FOV: 24 × 24 cm, 38 mm slice thickness, 36 slices, multi-slice mode: interleaved). Tasks were presented during fMRI using Presentation® software (Version 18.0, Neurobehavioral Systems, Inc., 2019, Berkeley, CA, www.neurojobs.com) in a counterbalanced order. The sMRI scan was acquired using a T1-MPRAGE sequence (TR: 1900 msec, TE: 3.09 msec, flip angle: 10°, FOV: 24 × 24 cm, 1 mm slice thickness, 144 slices, muli-slice mode: single shot).

2.5. Image processing and data analysis

See Fig. 1 for a flowchart of analysis procedures. The fMRI data from each subject were processed using AFNI (v16.2.16; Cox, 1996: afni.nimh.nih.gov). Preprocessing was done on a single-subject basis. The first three TRs were removed from each time course. Then, 3dDespike was applied to smooth spikes in signal over the time course. Next, time courses were shifted for each voxel to be aligned to the same temporal origin by detrending then interpolating the time series. Volumes across the time series were then aligned to the base volume and to the skull-stripped anatomy of the subject, then warped to standard Talairach space using the non-linear warping procedure 3dNwarpApply. Finally, each volume was blurred with a 4-mm full-width at half-maximum Gaussian smoothing kernel. For the task-fMRI data, TRs where the motion derivative value was 0.3 mm/TR or higher were censored from future analysis and stimuli onset times were regressed to identify signal associated with each condition, with demeaned motion parameters and their derivatives regressed to remove variance associated with movement. In rest data, individual data with an average motion derivative value of 0.3 mm/TR or higher ($n = 5$), with > 3% of TRs being

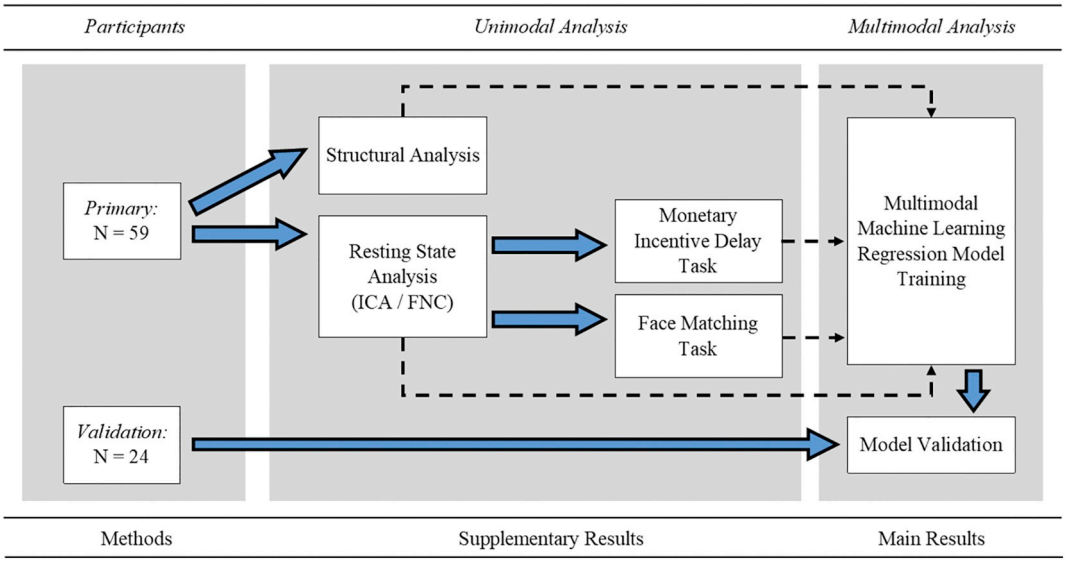

Fig. 1. Analysis pipeline.
Notes: Structural and resting state analyses were conducted on the subjects following the described procedures. Masks of resting state derived networks were used in the task analyses. Then machine learning regression algorithm was trained using features from structural, resting state, and task analyses. A separate sample was used for validation of the machine learning algorithm after training. Results from unimodal analyses are presented in Supplemental materials.

identified as above that cut off ($n = 2$), or with > 50 TRs having motion were removed prior to group level analysis. Additional control for nuisance variables occurred as part of the independent components analysis (ICA) procedure, described below, which identified and extracted signal due to sources such as motion or physiologic noise. Individual masks and registrations across modality were visually inspected to ensure quality and several additional subjects were removed from the analysis (MID: n = 2, Face: $n = 3$; final subjects: rs-fMRI, $n = 52$, sMRI, $n = 59$, MID $n = 57$, Face Matching $n = 56$).

The rs-fMRI data were analyzed using ICA in the GIFT (v3.0b) toolbox in SPM 12 after the preprocessing described above (Ashburner et al., 2014; Calhoun, 2004: mialab.mrn.org/software/gift/). ICA is a data-driven technique that extracts maximally different independent sources from signal data. It concatenates data across the time series, extracting networks of related fluctuating activity. In the primary sample, group ICA was used to extract 75 component time series using a PCA based separation algorithm at a single-subject level. Then a group PCA step was run to reduce the data to a single set of components for the group. Single-subject time courses for each group IC were back-reconstructed using the GICA3 algorithm.

ICs were reviewed manually, and 31 components were identified as noise related and removed. Resulting independent components (ICs) were labeled using the Component Labeling toolbox within GIFT, where the label was generated based on correlation with Resting State Network mask. Based on our a priori hypotheses, ICs labeled anterior salience network (ASN), posterior salience network (PSN), dorsal Default Mode Network (dDMN), ventral Default Mode Network (vDMN), left or right Executive Control Network (ECN), or basal ganglia (BG) were identified. Following all data selection procedures, rs-fMRI data from the validation sample was processed by back-reconstructing subject data into the already defined component space using the GIG-ICA algorithm. Between component functional network connectivity (FNC) was also examined. This procedure correlated the time courses of each IC with each other, creating a matrix of component connectivity. This matrix was calculated individually for each subject, based on back-reconstructed component data. See Supplemental Material 1 for unimodal analysis methods and results.

sMRI data were analyzed using Freesurfer (version 5.3.0; Fischl, 2012: surfer.nmr.mgh.harvard.edu). We used an auto-segmentation procedure on individual subjects based on the standard Freesurfer and Destrieux atlases to measure gray matter volume of structures (Destrieux et al., 2010; Fischl et al., 2002). The T1-MPRAGE sMRI scan was first conformed to 1 mm voxel size, resliced using trilinear interpolation, transformed to Talairach space, corrected for intensity non-uniformity using NU intensity correction (Sled et al., 1998), and skull stripped using a watershed algorithm and surface deformation process (Ségonne et al., 2004). Then auto-segmentation proceeded with labels assigned based on probabilistic location of structures. 10% of auto-segmented volumes were manually checked with recon_checker from FreeSurfer's QATools. This included checking for outliers, calculating signal-to-noise ratio, and visually examining generated snapshots of brain volume segmentation. From the auto-segmented regions, GMV from regions of interest (ROIs) were selected for inclusion in the analysis based on previous associations with AUD within selected networks of interest (ECN, SN, DMN, basal ganglia): the amygdala, hippocampus, ACC, PCC, NAcc, GP, caudate, putamen, thalamus, cerebellum, OFC, SFG, MFG, TPJ, temporal poles, anterior insula, and posterior insula. Right and left regions were extracted separately, as applicable. See Supplemental Material 2 for unimodal analysis methods and results.

Task-fMRI data was analyzed for the primary data set only using multivariate modeling (3dMVM) in AFNI. First, masks were created from the rest ICs described above (see Fig. 2A for a depiction of these masks). Each was used as a mask in 6 separate runs of 3dMVM. For each mask, the full MVM ([AUDIT + age + IQ + education + gender]*condition) was run for overall significance for all main effects and interactions. Then, conditions of interest were modeled using general linear tests and related to AUDIT score. For the MID task-fMRI, our conditions of interest were *Reward Anticipation* (High Reward – Neutral) and *Loss Anticipation* (High Loss – Neutral). Percentage of hits for reward and loss cued targets was examined behaviorally. In the Face Matching task-fMRI, our condition of interest was *Negative Emotional Face Processing* ([Angry Faces + Sad Faces + Fearful Faces]/3 – Neutral Faces). See Supplemental Material 3 for results from these unimodal analyses.

We then used a machine learning procedure trained in a subsample of our subjects to predict AUDIT score based on neural features. The inputs to these learning models were neural features extracted from the

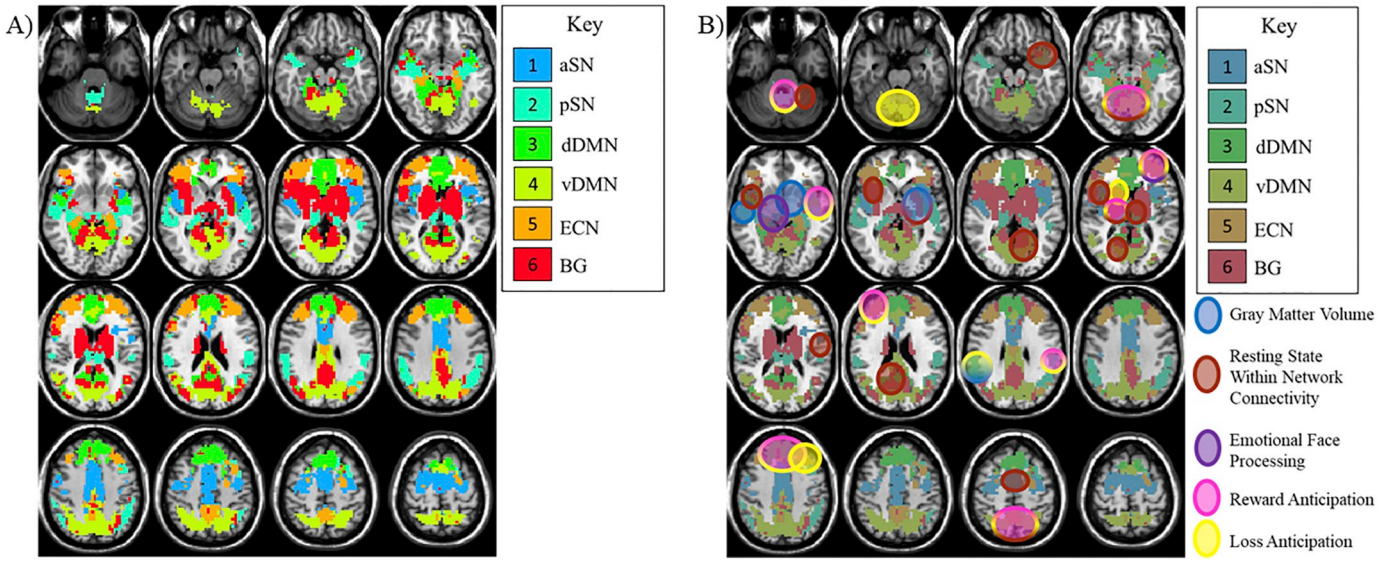

Fig. 2. Resting State Derived Network Masks and Corresponding Task Results by AUDIT.
Notes: A) Combinations of components extracted from the ICA analysis of resting state fMRI that corresponded to hypothesized alcohol-related regions. These masks were used in the task-based analyses. B) Circles indicate locations of rest condition, task condition, and structural effects of AUDIT score, and their overlap. Gradients indicate localization of more than one effect.

rs-fMRI, task-fMRI, and sMRI analyses. For rs-fMRI, beta coefficients within 5 mm radius spheres of locations in ICs related to AUDIT (based on the primary sample only) were extracted and included as within-network connectivity features. FNC connectivity matrices for each subject were also included as between-network connectivity features. For task-fMRI data, peak beta coefficients within 5 mm radius spheres of locations of AUDIT*condition effects (defined based on primary sample only) at a per-voxel p-value threshold of $p = .05$ were extracted and included as task-fMRI features. The beta-coefficients were also extracted at these locations in the validation sample. This uncorrected p-value was used for feature selection only, not for evaluation of statistical significance. Behavioral data was not included because there was not a significant correlation between AUDIT and hit percentages for reward or loss cued targets in the primary sample. For sMRI data, volumes of ROIs, described in the preceding paragraph, were included as features. The overlap between these features was evaluated qualitatively.

Within the initial sample that had data for all fMRI and sMRI scans ($n = 44$), we used 10 repeats of a 10-fold cross validation procedure to train a fast implementation random forest regression tree model through the 'ranger' method using the caret package in R (Kuhn, 2017; Wright and Ziegler, 2017). This model generated 500 trees and was tuned (tunelength = 10) in each iteration across number of randomly selected predictors, tree split rule (variance or extra trees), and minimum node size; by default, maximum tree depth was set to unlimited while other options (probability, replace, scale.permutation.importance, keep.inbag, houldout, quantreg, save.memory) are set to FALSE. Feature importance was evaluated using an impurity measure based on standardized response variance in prediction of AUDIT across trees. This feature importance was then normalized such that the feature with the maximum importance is scaled to 100. The optimum model was selected based on minimizing Root-Mean-Square Error (RMSE). We also report R^2 as a goodness of fit measure (calculated as the squared correlation between the predicted and observed AUDIT scores). The significance of the R^2 values was evaluated using a permutation testing procedure in which we compare the observed R^2 with a distribution of R^2 values generated based on 2000 random permutations of the sample data. The number of simulated R^2 values that were as or more extreme than the observed R^2 was divided by the number of simulations to produce a p-value for determining significance.

Then, the capacity of that model to generalize was tested using the validation data set ($n = 24$), which was not used in any way to determine which features were included in the models, providing us an estimate of the true error and performance of the model. This procedures follows recommendations by Shalev-Shwartz and Ben-David (2014). Demographic features included were age, IQ, years of education, and gender; we selected these features to serve as a baseline comparison model to aid in understanding the utility of the neuroimaging feature sets above features that could be more easily and affordably collected in primary care or hospital settings. In order to evaluate the relative performance of rs-fMRI, task-fMRI, sMRI, and demographic features, five versions of these models were trained, tested, and then compared: all neural features in combination (#features = 5653), just rs-fMRI features (#features = 922), just task-fMRI features (#features = 4699), just sMRI features (#features = 32), and just demographic features (#features = 4).

3. Results

3.1. Machine learning prediction analysis

For the rs-fMRI feature set, the optimum model across resamples in the primary data performed with an R^2 of .987 (mean[R^2] = 0.330, sd [R^2] = .308, RMSE = 4.64, $p < 5E\text{-}04$). In the validation data set, that model performed with an R^2 of .332 (RMSE = 8.04, $p = .007$). This was the best performing model overall. Features representing within-network basal ganglia connectivity and between-network connectivity features spanning the brain were important for predicting AUDIT score. This included connectivity between hypothesized SN, DMN, ECN, and BG networks as well as visual, sensorimotor, auditory, and language networks; See Table 2 for a specific list of features. When applying a Bonferroni correction to account for the five feature sets compared ($_{pbonferroni} = p_{uncorrected}/5$), results remained significant.

Table 2
20 Most Important Features Ranked by Importance from Resting State Functional Connectivity Feature Random Forest Model of AUDIT Total Score.

Feature Info	Impurity
Within-Network Connectivity: BG (left)	100
FNC: ASN — Sensorimotor Network	79.32
FNC: vDMN — vDMN (extending dorsally)	77.02
FNC: ASN — PSN	71.68
FNC: vDMN — Auditory Network	71.3
FNC: ASN — Visuospatial Network	70.66
FNC: Lateral vDMN — Medial vDMN	69.59
FNC: dDMN — ECN (left)	67.78
FNC: vDMN — Primary Visual Network	67.71
FNC: Visuospatial Network — Language Network	66.91
FNC: PSN — Visuospatial Network	66.71
FNC: vDMN — PSN	65.22
FNC: ECN (right) — Sensorimotor Network	65.04
FNC: Visuospatial Network — Auditory Network	64.08
FNC: vDMN — Higher Visual Network	63.84
FNC: dDMN — Higher Visual Network	63.58
FNC: BG — Sensorimotor Network	63.15
FNC: BG — Auditory Network	62.63
FNC: vDMN — Primary Visual Network	62.46
FNC: PSN — Higher Visual Network	62.2

Notes: Impurity is a standarized value based on response variance across regression trees; the scale is 0 to 100. The distribution of these index scores is plotted below. FNC: Features from the resting state fMRI analysis of functional network connectivity, where — indicates a between-network connection; v/dDMN: ventral/dorsal default mode network; A/PSN: anterior/posterior salience network; BG: basal ganglia network; ECN: executive control network.

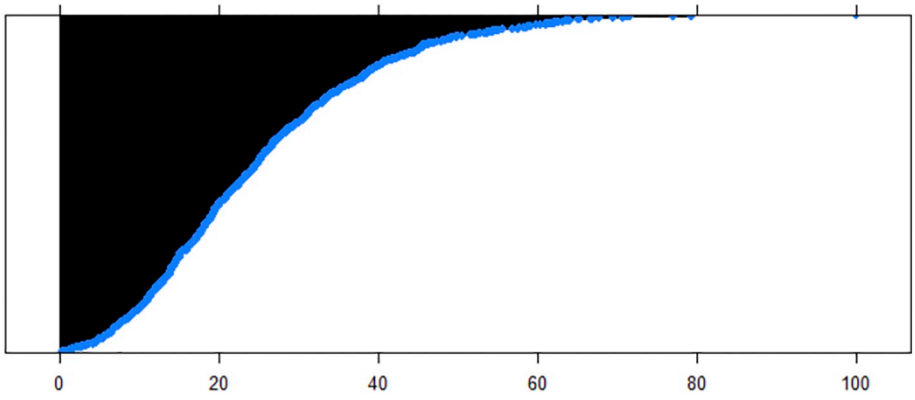

In the combined feature set, task-fMRI feature only set, sMRI feature only set, and demographic feature only set for the primary data, the optimum model did not perform significantly worse or better than in the rs- fMRI feature set and explained a significant portion of the varience of AUDIT (combined set: mean[R^2] = 0.339, sd[R^2] = 0.311, R^2 = .995, RMSE = 3.550, p < 5E-04; task-fMRI only: mean [R^2] = 0.365, sd[R^2] = 0.310, R^2 = .992, RMSE = 3.15, p < 5E-04; sMRI *only*: mean[R^2] = 0.332, sd[R^2] = 0.304, R^2 = .965, RMSE = 4.634, p < 5E-04; demographic only: mean[R^2] = 0.380, sd [R^2] = 0.323, R^2 = .869, RMSE = 9.76, p < 5E-04; all p_{diff} = 1); however, when the capacity of these models to generalize were tested in the validation set, the R^2 and RMSE values were non-significant (combined set: R^2 = .004, RMSE = 8.36, p = 0.773; task-fMRI only: R^2 = .093, RMSE = 8.63, p = 0.152; sMRI only: R^2 = .003, RMSE = 8.11, p = 0.793; demographic only: R^2 = .012, RMSE = 9.76, p = 0.617), explaining 32.8%, 23.9%, 32.9% and 32.0% less variance than the rs-fMRI feature model, respectively. See Fig. 3 for a visual depiction of the relationship between important features and AUDIT total score in both the primary and validation samples.

3.2. Combined data set

The overlap between unimodal effects of AUDIT score within the resting state networks was evaluated qualitatively for the purposes of further understanding the unique and shared contributions of each modality (see Fig. 2B). Individual unimodal results are reported in Supplementary Materials. AUDIT score was related to atypical engagement of right ECN across all three functional processes. Atypical engagement corresponded to a negative or positive association between AUDIT and brain measures, but differed in magnitude or directionality depending on the modality. Atypical vDMN and lentiform BG engagement related to AUDIT score was specific to anticipation of loss, while AUDIT effects on reward/loss anticipation overlapped in the PSN, dDMN, and left ECN. Thalamic BG and vDMN engagement was related to AUDIT score for both reward/loss anticipation and rs-fMRI connectivity, but other effects of AUDIT in portions of the DMN, ASN, and left BG were specific to rs-fMRI connectivity. sMRI atypicalities related to AUDIT in PSN corresponded to functional abnormalities associated with loss anticipation, while AUDIT effects on right BG network structure corresponded to rs-fMRI connectivity. Otherwise, left temporal PSN effects of AUDIT were found specifically in sMRI measures.

4. Discussion

In this study, we used rs-fMRI, fMRI tasks of emotional face processing and monetary incentive delay, and sMRI to predict AUD severity, as measured by the AUDIT. We also considered the relative predictive utility of using different combinations of these neural features. We found that in an independent sample, rs-fMRI connectivity features best predict AUD severity, although task-fMRI based neural engagement, GMV, and demographic traits can be used to account for variance in AUD severity in a training sample.

We found support for our hypothesis that neural features corresponding to the SN, DMN, ECN, and BG would predict AUDIT score. We found that rs-fMRI-based within and between network connectivity features involving these network components contributed strongly to prediction models of AUDIT score, and that this model explained 33% of variance in a naïve sample. Although this still leaves substantial unaccounted for variance, it is important to consider that conventional laboratory tests perform in the “fail” to “poor” range in diagnosing AUD (Aertgeerts et al., 2001). For further comparison purposes, a random forest model trained on demographic features (age, IQ, years of education, and gender) only accounted for 1.2% of the variance in the validation sample.

The ability to use neural data to indicate AUD severity can be beneficial in medical settings to understand disorder severity without

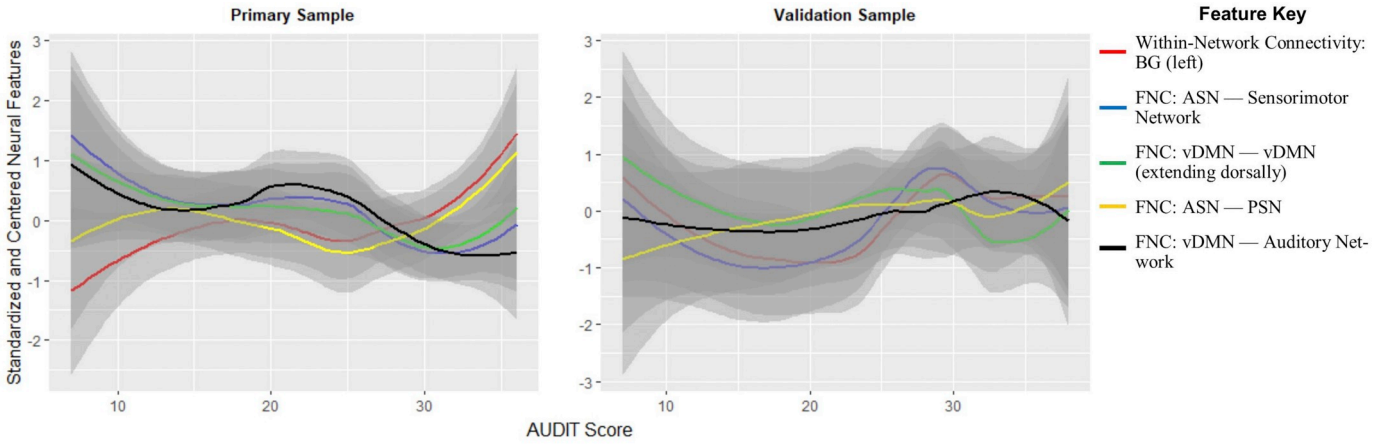

Fig. 3. Association between AUDIT total score and resting state connectivity variables of importance.

depending on self-report. The AUDIT is clinically useful for diagnosis of heavy alcohol drinking, AUD, harmful use, binge drinking (Reinert and Allen, 2007), intimate partner violence (Foran and O'Leary, 2008), social problems, and alcohol-related medical disorders/hospitalizations (Conigrave et al., 1995b). However, clinical utility is limited by the potential incentive to misrepresent alcohol use. Studies report stigma associated with AUD, finding that the general public thinks individuals with AUD are less desirable to work or socialize with, and are more likely to be violent (Pescosolido et al., 2010). A neural diagnostic tool would help to address this limitation.

Another important implication of these findings is support for the cycle of addiction model of addiction neurobiology (2016). We used data from networks put forward by that model and found a neural basis corresponding to alcohol misuse. Specifically, we found that neural activity at rest corresponding to the preoccupation/anticipation (ECN/SN), withdrawal/negative affect (DMN), and binge/intoxication (SN/BG) neurocircuitry, particularly connections therein, predicted AUD severity, suggesting that more severe alcohol use is related to differential neural engagement, structure, or connectivity within those systems.

We did not find support for our hypothesis that rs-fMRI, task-fMRI, and sMRI features combined would perform better than any set of features on their own in predicting AUDIT score. Within our primary data set, we did not see a significant difference between models. However, in the validation sample where we tested the capacity of our models to generalize, we saw a notable performance advantage from rs-fMRI connectivity feature model. This suggests that rs-fMRI derived features lend themselves to a more stable prediction model that translates to a new sample more effectively. These features represent intrinsic network connectivity at rest without outside stimulation; however, it is possible that variability in this network connectivity could be due to sleep states rather than resting states, despite directions to participants to stay awake (Haimovici et al., 2017; Tagliazucchi and Laufs, 2014).

One reason that could explain why the combined model was not the optimum model, as we predicted, is that the additional features lead to overfitting the model in the training process. However, this is not the first evidence of the importance of functional connectivity during rs-fMRI as a biomarker; rs-fMRI has been previously found to be a neural indicator of disease and mental health. For example, DMN engagement during rest differentiates Alzheimer's disease from normal aging (Greicius et al., 2004). Resting state neural dynamic differences have also been associated with depression, autism, and schizophrenia (Cherkassky et al., 2006; Sheline et al., 2010; Skudlarski et al., 2010; Zhou et al., 2007). Some work challenges the role of rs-fMRI as useful above and beyond specific task-fMRI (Morcom and Fletcher, 2007); our finding that rs-fMRI features perform better than task-fMRI, sMRI or even basic demographic information in predicting AUD severity runs counter to that. Given this, standard clinical MRI scan protocols may be improved by the addition of a rs-fMRI scan, which takes 5–10 min to collect (Van Dijk et al., 2010) and doesn't require complex tasks, training, or stimulus presentation software (Takamura and Hanakawa, 2017). Rs-fMRI is also fairly stable across time: for example Chou et al., report intraclass correlation of $> .60$ between nine rs-fMRI scans over a year (Chou et al., 2012).

Unexpectedly, connectivity with visual, visual association, and sensorimotor regions of the brain was important for predicting AUD severity. Previous work has demonstrated similar relationships between alcohol use and visual system activity. In one study, AUDIT was negatively related to functional network connectivity during rest between fusiform areas and post-central gyrus/cuneus areas, and between the inferior occipital gyrus and the supplementary motor area (Vergara et al., 2017). Claus et al. (2011b) found that the precuneus/lateral occipital cortex activity was positively associated with years of heavy drinking in response to alcohol taste cues, reflecting increased motivation and attention towards salient stimuli. Our supplementary finding that engagement of occipitoparietal regions during reward anticipation is associated with AUD severity suggests this motivation bias affects monetary processing as well.

The unimodal analyses done as the first step of our procedure only partially replicated the results of previous studies. See Supplemental Material 4 for a discussion of these findings. However, there are important differences to our subjects and procedures that may explain these differences. All participants in our sample are moderate to heavy alcohol users while most studies in this field examine AUD dichotomously. Moreover, the mechanisms associated with chronic versus acute alcohol administrations differ; a biomarker important for diagnosis may not also vary with severity. The effects of severity within an AUD sample may also be smaller than group differences. In emotional face processing and sMRI studies here, replication was only seen at lower thresholds, possibly indicating that our sample was underpowered to detect effects of severity on these neural measures. Further, previous studies did not consistently control for demographic variables like age, IQ, and gender, which are related to brain structure (Andreasen et al., 1993; Gur et al., 1999; Hommer et al., 2001; Sussman et al., 2019). These variables may also interact with AUD; older individuals have increased neural vulnerability to alcohol misuse (Pfefferbaum et al., 1992), IQ is impacted by and predicts chronic alcohol use (Schottenbauer et al., 2007), and educated individuals are less likely to drink heavily (Ross and Wu, 1995). In our sample, AUDIT and age interacted in association with rs-fMRI connectivity and age was the most important demographic predictor of AUDIT, further emphasizing the need to consider covariates in these analyses.

4.1. Limitations

Despite the potential clinical utility of neural data as predictive of AUD severity, there are still major steps to take prior to such an applied use. First, this study has a small sample for training and further testing a prediction model. This is likely reflected in the large variability in the R^2 values across training folds. Random forest models are able to handle a low ratio of observations to parameters as is present in this data set (Matsuki et al., 2016), although such a sample size here may still leave the model vulnerable to overfitting, given the large number of features included. In order to address this, we ran a supplementary model in which we changed model selection criteria during training to follow Breiman's 1SE rule, favoring shallower trees and thus, less likely to overfit (Breiman, 2017). This did not reduce indicators of potential overfitting (i.e., R^2 values for the primary sample increased or did not substantively change; R^2 values in the validation sample dropped or did not substantively change). Moreover, the risk of overfitting a model is that the model fits random noise and variation specific to the training sample rather than to the population the model is designed to estimate. However, by using cross-validation within development of the model in the primary sample, and further testing the model with a separate validation sample, we address this concern by reporting the models' abilities to generalize to another subsample of the population. We do emphasize the need to focus on the results from the validation sample and interpret cautiously findings from the primary sample (i.e., the feature importance rankings), as the latter are not tested for generalizability. Further, given these limitations and since we do not have an estimate of the variability of the generalizability, there is need for replication in additional independent samples.

Although the best preforming (rs-fMRI feature) model explains a notable percentage of the variance associated with AUD severity, > 60% remains for other factors. A portion of that may be unexplainable, but demographic features, individual differences, genetics, and family dynamics may contribute to prediction of alcohol use severity and outcomes (Behrendt et al., 2017; Oslin et al., 2003; Rosenström et al., 2017; Umut et al., 2017). Although demographic/behavioral variables (i.e., age, IQ, gender, years of education, smoking) were not significantly related to AUDIT in our sample, AUD individuals tend to differ from non-substance using individuals on many of these traits. It is also possible that some of the variance the model does account for is related to traits such as smoking or comorbid substance use, particularly considering previous work demonstrates shared and independent connectivity correlates in smokers who do or do not also use alcohol (Vergara et al., 2017). However, we do not believe this is what is driving our results since these factors were not significantly related to AUDIT total score. Moreover, comorbid tobacco and illicit drug use is characteristic of the population we hope to generalize to; > 50% of heavy drinkers also use tobacco products, and about 11% of drinkers also use illicit drugs (SAMHSA, 2017). Additional studies should be done in an effort to determine whether machine learning techniques such as this can be used to distinguish between types of substance use disorders.

Manual selection of features based on unimodal analysis and a priori hypotheses was done in the primary sample prior to running machine learning analysis. Given the small size of our sample, the risk of overfitting, and the potential number of features available in neuroimaging data, this was done to minimize the number of features and noise in the models. In order to minimize the potential bias this could introduce in generalizability, our validation sample was independent of these unimodal analyses. We do not believe that such a potential bias is driving our results. If our results were driven by the bias, we would anticipate that the rest-feature model would have the worst generalizability, since the majority of these features were agnostically rather than manually pruned. In fact, the rest-only feature set model performed the best out of all the models. Regardless, additional care—such as replication in an independent sample—should be taken prior to approaching this as a clinical tool.

Limitations involved in feature selection across modalities may also have influenced the comparison between modalities. In order to limit these concerns, identical network masks were applied to within network rs-fMRI and task-fMRI imaging. However, the ICA-derived functional networks do not map directly on to brain structures. As a result, structures thought to contribute to the ECN, SN, basal ganglia, and DMN networks, including those regularly found in previous studies of AUD, were used. This might mean that the sMRI features capture slightly different information than the functional feature set. A model trained and validated using different structural and functional features, then, might have different relative predictive value than the findings seen here. Because of this, and because of the discrepancies between the number of features included in each set, the relative poor performance of the other modalities in comparison to rs-fMRI should be interpreted cautiously (Varoquaux, 2018).

Additionally, it is unclear if the neural features identified as predictive here are pre-existing risk factors or caused by chronic alcohol use. A longitudinal study is required to understand this potential causality. The risks associated with false-diagnosis (stigma, self-fulfilling prophecies) should be considered carefully, especially before using these features prospectively.

5. Conclusions

Overall, this is an important step towards the utility of neuroimaging to inform treatment and early identification of AUD. Additional work is necessary to understand how these neural features relate to treatment efficacy, disorder prognosis, and relapse. For example, conversion from mild cognitive impairment to Alzheimer's disease can be predicted with an accuracy of 86% using multimodal neuroimaging data (Kebets et al., 2015); a similar understanding of AUD trajectory based on neural features could be derived from a prospective study of younger individuals with mild AUD. Other studies found that neural engagement predicted relapse in methamphetamine users post-treatment at a rate of 90.4% (Paulus et al., 2005) and that anterior cingulate connectivity during response inhibition predicted substance use treatment at a rate of 79.7% (Steele et al., 2018); such a study in AUD could inform treatment completion, treatment plans, and identify individuals most highly at risk for relapse. Ultimately, this may allow for development of clinically useful neuroimaging biomarkers to optimize treatment for and prevention of AUD and related negative drinking consequences.

Acknowledgements

This research was supported by the National Institutes of Alcohol Abuse and Alcoholism/National Institutes of Health intramural research funding ZIA-AA000125 to the Clinical NeuroImaging Research Core (PI: R. Momenan). Portions of these findings were presented at the 2018 meetings of the Society of Biological Psychiatry and the Organization for Human Brain Mapping.

The raw data supporting the conclusions of this manuscript will be made available by the authors, without undue reservation, to any qualified researcher.

Author contributions

SF, SD, EG, and RM conceptualized and contributed intellectually to the analysis and interpretation of results reported here. RM served as the principal investigator for the protocol under which the data was collected. ND served as the principal investigator for the protocol under which the screening data was collected. SD was primarily involved in data collection and conducted data cleaning and analysis. SF conducted data analysis and wrote the manuscript. EG & RM provided revisions and modifications of the manuscript. All authors approved a final version of the manuscript.

Conflict of interest statement

None.

Declarations of interest

None.

Appendix A. Supplementary data

Supplementary data to this article can be found online at https://doi.org/10.1016/j.nicl.2019.101782.

References

Aertgeerts, B., Buntinx, F., Ansoms, S., Fevery, J., 2001. Screening properties of questionnaires and laboratory tests for the detection of alcohol abuse or dependence in a general practice population. Br. J. Gen. Pract. 51 (464), 206–217.

Ames, S.L., Wong, S.W., Bechara, A., Cappelli, C., Dust, M., Grenard, J.L., Stacy, A.W., 2014. Neural correlates of a Go/NoGo task with alcohol stimuli in light and heavy young drinkers. Behav. Brain Res. 274, 382–389. https://doi.org/10.1016/j.bbr.2014.08.039.

Andreasen, N.C., Flaum, M., Swayze 2nd, V., O'Leary, D.S., Alliger, R., Cohen, G., ... Yuh, W.T., 1993. Intelligence and brain structure in normal individuals. Am. J. Psychiatry 150 (1), 130.

Ashburner, J., Barnes, G., Chen, C., Daunizeau, J., Flandin, G., Friston, K., ... Moran, R., 2014. SPM12 Manual. Wellcome Trust Centre for Neuroimaging, London (UK).

Beck, A., Schlagenhauf, F., Wustenberg, T., Hein, J., Kienast, T., Kahnt, T., ... Wrase, J., 2009. Ventral striatal activation during reward anticipation correlates with impulsivity in alcoholics. Biol. Psychiatry 66 (8), 734–742. https://doi.org/10.1016/j.biopsych.2009.04.035.

Behrendt, S., Buhringer, G., Hofler, M., Lieb, R., Beesdo-Baum, K., 2017. Prediction of incidence and stability of alcohol use disorders by latent internalizing psychopathology risk profiles in adolescence and young adulthood. Drug Alcohol Depend. 179, 32–41. https://doi.org/10.1016/j.drugalcdep.2017.06.006.

Breiman, L., 2017. Classification and Regression Trees. Routledge.

Calhoun, V., 2004. Group ICA of fMRI Toolbox (GIFT). Online at. http://icatb.sourceforge.net.

Camchong, J., Stenger, V.A., Fein, G., 2013a. Resting-state synchrony during early alcohol abstinence can predict subsequent relapse. Cereb. Cortex 23 (9), 2086–2099. https://doi.org/10.1093/cercor/bhs190.

Camchong, J., Stenger, V.A., Fein, G., 2013b. Resting-state synchrony in short-term versus long-term abstinent alcoholics. Alcohol. Clin. Exp. Res. *37* (5), 794–803. https://doi.org/10.1111/acer.12037.

Chanraud, S., Pitel, A.L., Pfefferbaum, A., Sullivan, E.V., 2011. Disruption of functional connectivity of the default-mode network in alcoholism. Cereb. Cortex 21 (10), 2272–2281. https://doi.org/10.1093/cercor/bhq297.

Charlet, K., Schlagenhauf, F., Richter, A., Naundorf, K., Dornhof, L., Weinfurtner, C.E.J., ... Heinz, A., 2014. Neural activation during processing of aversive faces predicts treatment outcome in alcoholism. Addict. Biol. 19 (3), 439–451. https://doi.org/10.1111/adb.12045.

Cherkassky, V.L., Kana, R.K., Keller, T.A., Just, M.A., 2006. Functional connectivity in a baseline resting-state network in autism. Neuroreport 17 (16), 1687–1690. https://doi.org/10.1097/01.wnr.0000239956.45448.4c.

Chou, Y.-h., Panych, L.P., Dickey, C.C., Petrella, J.R., Chen, N.-K., 2012. Investigation of long-term reproducibility of intrinsic connectivity network mapping: a resting-state fMRI study. Am. J. Neuroradiol. 33 (5), 833–838.

Claus, E.D., Hutchison, K.E., 2012. Neural mechanisms of risk taking and relationships with hazardous drinking. Alcohol. Clin. Exp. Res. 36 (6), 408–416. https://doi.org/10.1111/j.1530-0277.2011.01694.x.

Claus, E.D., Ewing, S.W.F., Filbey, F.M., Sabbineni, A., Hutchison, K.E., 2011a. Identifying neurobiological phenotypes associated with alcohol use disorder severity. Neuropsychopharmacology 36 (10), 2086–2096.

Claus, E.D., Kiehl, K.A., Hutchison, K.E., 2011b. Neural and behavioral mechanisms of impulsive choice in alcohol use disorder. Alcohol. Clin. Exp. Res. 35 (7), 1209–1219. https://doi.org/10.1111/j.1530-0277.2011.01455.x.

Conigrave, K.M., Hall, W.D., Saunders, J.B., 1995a. The AUDIT questionnaire: choosing a cut-off score. Alcohol Use Disorder Identification Test. Addiction 90 (10), 1349–1356.

Conigrave, K.M., Saunders, J.B., Reznik, R.B., 1995b. Predictive capacity of the audit questionnaire for alcohol-related harm. Addiction 90 (11), 1479–1485. https://doi.org/10.1111/j.1360-0443.1995.tb02810.x.

Cox, R.W., 1996. AFNI: software for analysis and visualization of functional magnetic resonance neuroimages. Comput. Biomed. Res. 29 (3), 162–173.

Cservenka, A., Casimo, K., Fair, D.A., Nagel, B.J., 2014. Resting state functional connectivity of the nucleus accumbens in youth with a family history of alcoholism. Psychiatry Res. Neuroimag. 221 (3), 210–219. https://doi.org/10.1016/j.pscychresns.2013.12.004.

Destrieux, C., Fischl, B., Dale, A., Halgren, E., 2010. Automatic parcellation of human cortical gyri and sulci using standard anatomical nomenclature. NeuroImage 53 (1), 1–15. https://doi.org/10.1016/j.neuroimage.2010.06.010.

Du, W., Calhoun, V.D., Li, H., Ma, S., Eichele, T., Kiehl, K.A., ... Adali, T., 2012. High classification accuracy for schizophrenia with rest and task fMRI data. Front. Hum. Neurosci. 6, 145. https://doi.org/10.3389/fnhum.2012.00145.

Epstein, E.E., Labouvie, E., McCrady, B.S., Jensen, N.K., Hayaki, J., 2002. A multi-site study of alcohol subtypes: classification and overlap of unidimensional and multidimensional typologies. Addiction 97 (8), 1041–1053.

Esposito, F., Pignataro, G., Di Renzo, G., Spinali, A., Paccone, A., Tedeschi, G., Annunziato, L., 2010. Alcohol increases spontaneous BOLD signal fluctuations in the visual network. NeuroImage 53 (2), 534–543. https://doi.org/10.1016/j.neuroimage.2010.06.061.

Fein, G., Sclafani, V., Cardenas, V., Goldmann, H., Tolou-Shams, M., Meyerhoff, D.J., 2002. Cortical gray matter loss in treatment-naive alcohol dependent individuals. Alcohol. Clin. Exp. Res. 26 (4), 558–564.

Filbey, F.M., Claus, E., Audette, A.R., Niculescu, M., Banich, M.T., Tanabe, J., Hutchison, K.E., 2008. Exposure to the taste of alcohol elicits activation of the mesocorticolimbic neurocircuitry. Neuropsychopharmacology 33 (6), 1391–1401. https://doi.org/10.1038/sj.npp.1301513.

Fink, B.C., Steele, V.R., Maurer, M.J., Fede, S.J., Calhoun, V.D., Kiehl, K.A., 2016. Brain potentials predict substance abuse treatment completion in a prison sample. Brain Behav. 6 (8), e00501.

Fischl, B., 2012. FreeSurfer. NeuroImage 62 (2), 774–781.

Fischl, B., Salat, D.H., Busa, E., Albert, M., Dieterich, M., Haselgrove, C., ... Klaveness, S., 2002. Whole brain segmentation: automated labeling of neuroanatomical structures in the human brain. Neuron 33 (3), 341–355.

Foran, H.M., O'Leary, K.D., 2008. Alcohol and intimate partner violence: a meta-analytic review. Clin. Psychol. Rev. 28 (7), 1222–1234. https://doi.org/10.1016/j.cpr.2008.05.001.

Gilman, J.M., Hommer, D.W., 2008. Modulation of brain response to emotional images by alcohol cues in alcohol-dependent patients. Addict. Biol. 13 (3–4), 423–434. https://doi.org/10.1111/j.1369-1600.2008.00111.x.

Greicius, M.D., Srivastava, G., Reiss, A.L., Menon, V., 2004. Default-mode network activity distinguishes Alzheimer's disease from healthy aging: evidence from functional MRI. Proc. Natl. Acad. Sci. U. S. A. 101 (13), 4637–4642. https://doi.org/10.1073/pnas.0308627101.

Grodin, E.N., Lin, H., Durkee, C.A., Hommer, D.W., Momenan, R., 2013. Deficits in cortical, diencephalic and midbrain gray matter in alcoholism measured by VBM: effects of co-morbid substance abuse. NeuroImage 2, 469–476.

Gur, R.C., Turetsky, B.I., Matsui, M., Yan, M., Bilker, W., Hughett, P., Gur, R.E., 1999. Sex differences in brain gray and white matter in healthy young adults: correlations with cognitive performance. J. Neurosci. 19 (10), 4065–4072.

Haimovici, A., Tagliazucchi, E., Balenzuela, P., Laufs, H., 2017. On wakefulness fluctuations as a source of BOLD functional connectivity dynamics. Sci. Rep. 7 (1), 5908.

Hariri, A.R., Mattay, V.S., Tessitore, A., Kolachana, B., Fera, F., Goldman, D., ... Weinberger, D.R., 2002. Serotonin transporter genetic variation and the response of the human amygdala. Science 297 (5580), 400–403.

Heatherton, T.F., Kozlowski, L.T., Frecker, R.C., FAGERSTROM, K.O., 1991. The Fagerström test for nicotine dependence: a revision of the Fagerstrom Tolerance Questionnaire. Addiction 86 (9), 1119–1127.

Heinz, A., Siessmeier, T., Wrase, J., Hermann, D., Klein, S., Grüsser-Sinopoli, S.M., ... Gründer, G., 2004. Correlation between dopamine D2 receptors in the ventral striatum and central processing of alcohol cues and craving. Am. J. Psychiatr. 161 (10), 1783–1789.

Hommer, D.W., Momenan, R., Kaiser, E., Rawlings, R.R., 2001. Evidence for a gender-related effect of alcoholism on brain volumes. Am. J. Psychiatr. 158 (2), 198–204.

Kebets, V., Richiardi, J., Van Assche, M., Goldstein, R., van der Meulen, M., Vuilleumier, P., ... Assal, F., 2015. Predicting pure amnestic mild cognitive impairment conversion to alzheimer's disease using joint modeling of imaging and clinical data. In: Paper Presented at the Pattern Recognition in NeuroImaging (PRNI), 2015 International Workshop on.

Kelly, A.M.C., Uddin, L.Q., Biswal, B.B., Castellanos, F.X., Milham, M.P., 2008. Competition between functional brain networks mediates behavioral variability. NeuroImage 39 (1), 527–537. https://doi.org/10.1016/j.neuroimage.2007.08.008.

Khalili-Mahani, N., Zoethout, R.M.W., Beckmann, C.F., Baerends, E., de Kam, M.L., Soeter, R.P., ... Rombouts, S., 2012. Effects of morphine and alcohol on functional brain connectivity during "resting state": a placebo-controlled crossover study in healthy young men. Hum. Brain Mapp. 33 (5), 1003–1018. https://doi.org/10.1002/hbm.21265.

Knutson, B., Adams, C., Fong, G., Walker, J., Hommer, D., 2001. Parametric FMRI confirms selective recruitment of nucleus accumbens during anticipation of monetary reward. NeuroImage 13 (6, Supplement), 430. https://doi.org/10.1016/S1053-8119(01)91773-2.

Koob, G.F., Volkow, N.D., 2016. Neurobiology of addiction: a neurocircuitry analysis. Lancet Psychiatry 3 (8), 760–773.

Kranzler, H.R., Kirk, J., 2001. Efficacy of naltrexone and acamprosate for alcoholism treatment: a meta-analysis. Alcohol. Clin. Exp. Res. 25 (9), 1335–1341.

Kuhn, M., 2017. caret: Classification and Regression Training (Version 6.0–77). Retrieved from. https://CRAN.R-project.org/package=caret.

Lei, X., Wang, Y.L., Yuan, H., Mantini, D., 2014. Neuronal oscillations and functional interactions between resting state networks: effects of alcohol intoxication. Hum. Brain Mapp. 35 (7), 3517–3528. https://doi.org/10.1002/hbm.22418.

Li, C.S.R., Luo, X., Yan, P., Bergquist, K., Sinha, R., 2009. Altered impulse control in alcohol dependence: neural measures of stop signal performance. Alcohol. Clin. Exp. Res. 33 (4), 740–750. https://doi.org/10.1111/j.1530-0277.2008.00891.x.

Matsuki, K., Kuperman, V., Van Dyke, J.A., 2016. The Random Forests statistical technique: an examination of its value for the study of reading. Sci. Stud. Read. 20 (1), 20–33.

Miller, W.R., Wilbourne, P.L., 2002. Mesa Grande: a methodological analysis of clinical trials of treatments for alcohol use disorders. Addiction 97 (3), 265–277.

Morcom, A.M., Fletcher, P.C., 2007. Does the brain have a baseline ? Why we should be resisting a rest. NeuroImage 37 (4), 1073–1082. https://doi.org/10.1016/j.neuroimage.2006.09.013.

Moss, H.B., Chen, C.M., Yi, H.-y., 2007. Subtypes of alcohol dependence in a nationally representative sample. Drug Alcohol Depend. 91 (2), 149–158.
Muller-Oehring, E.M., Jung, Y.C., Pfefferbaum, A., Sullivan, E.V., Schulte, T., 2015. The resting brain of alcoholics. Cereb. Cortex 25 (11), 4155–4168. https://doi.org/10.1093/cercor/bhu134.
Myrick, H., Anton, R.F., Li, X.B., Henderson, S., Drobes, D., Voronin, K., George, M.S., 2004. Differential brain activity in alcoholics and social drinkers to alcohol cues: relationship to craving. Neuropsychopharmacology 29 (2), 393–402. https://doi.org/10.1038/sj.npp.1300295.
Neurobehavioral Systems, I, 2019. Presentation Software (Version 18.0). Neurobehavioral Systems, Inc, Berkeley, CA Retrieved from. www.neurobs.com.
Oslin, D.W., Berrettini, W., Kranzler, H.R., Pettinati, H., Gelernter, J., Volpicelli, J.R., O'Brien, C.P., 2003. A functional polymorphism of the mu-opioid receptor gene is associated with naltrexone response in alcohol-dependent patients. Neuropsychopharmacology 28 (8), 1546–1552. https://doi.org/10.1038/sj.npp.1300219.
Paulus, M.P., Tapert, S.F., Schuckit, M.A., 2005. Neural activation patterns of methamphetamine-dependent subjects during decision making predict relapse. Arch. Gen. Psychiatry 62 (7), 761–768. https://doi.org/10.1001/archpsyc.62.7.761.
Pescosolido, B.A., Martin, J.K., Long, J.S., Medina, T.R., Phelan, J.C., Link, B.G., 2010. "A Disease Like Any Other"? A decade of change in public reactions to schizophrenia, depression, and alcohol dependence. Am. J. Psychiatr. 167 (11), 1321–1330. https://doi.org/10.1176/appi.ajp.2010.09121743.
Pfefferbaum, A., Lim, K.O., Zipursky, R.B., Mathalon, D.H., Rosenbloom, M.J., Lane, B., ... Sullivan, E.V., 1992. Brain gray and white matter volume loss accelerates with aging in chronic-alcoholics - a quantitative MRI study. Alcohol. Clin. Exp. Res. 16 (6), 1078–1089. https://doi.org/10.1111/j.1530-0277.1992.tb00702.x.
Qin, P.M., Northoff, G., 2011. How is our self related to midline regions and the default-mode network? NeuroImage 57 (3), 1221–1233. https://doi.org/10.1016/j.neuroimage.2011.05.028.
Rando, K., Hong, K.-I., Bhagwagar, Z., Li, C.-S.R., Bergquist, K., Guarnaccia, J., Sinha, R., 2011. Association of frontal and posterior cortical gray matter volume with time to alcohol relapse: a prospective study. Am. J. Psychiatr. 168 (2), 183–192.
Reinert, D.F., Allen, J.P., 2007. The alcohol use disorders identification test: an update of research findings. Alcohol. Clin. Exp. Res. 31 (2), 185–199. https://doi.org/10.1111/j.1530-0277.2006.00295.x.
Rosenström, T., Torvik, F.A., Ystrom, E., Czajkowski, N.O., Gillespie, N.A., Aggen, S.H., ... Reichborn-Kjennerud, T., 2017. Prediction of alcohol use disorder using personality disorder traits: a twin study. Addiction. https://doi.org/10.1111/add.13951. n/a-n/a.
Ross, C.E., Wu, C.L., 1995. The links between education and health. Am. Sociol. Rev. 60 (5), 719–745. https://doi.org/10.2307/2096319.
Sacks, J.J., Gonzales, K.R., Bouchery, E.E., Tomedi, L.E., Brewer, R.D., 2015. 2010 national and state costs of excessive alcohol consumption. Am. J. Prev. Med. 49 (5), e73–e79.
Salloum, J.B., Ramchandani, V.A., Bodurka, J., Rawlings, R., Momenan, R., George, D., Hommer, D.W., 2007. Blunted rostral anterior cingulate response during a simplified decoding task of negative emotional facial expressions in alcoholic patients. Alcohol. Clin. Exp. Res. 31 (9), 1490–1504.
SAMHSA, 2015. 2015 National Survey on Drug Use and Health (NSDUH).
SAMHSA, 2017. 2017 National Survey on Drug Use and Health (NSDUH).
Saunders, J.B., Aasland, O.G., Babor, T.F., Delafuente, J.R., Grant, M., 1993. Development of the alcohol-use disorders identification test (audit) - who collaborative project on early detection of persons with harmful alcohol-consumption. Addiction 88 (6), 791–804. https://doi.org/10.1111/j.1360-0443.1993.tb02093.x.
Schmaal, L., Goudriaan, A.E., Joos, L., Kruse, A.M., Dom, G., van den Brink, W., Veltman, D.J., 2013. Modafinil modulates resting-state functional network connectivity and cognitive control in alcohol-dependent patients. Biol. Psychiatry 73 (8), 789–795. https://doi.org/10.1016/j.biopsych.2012.12.025.
Schottenbauer, M.A., Momenan, R., Kerick, M., Hommer, D.W., 2007. Relationships among aging, IQ, and intracranial volume in alcoholics and control subjects. Neuropsychology 21 (3), 337–345. https://doi.org/10.1037/0894-4105.21.3.337.
Ségonne, F., Dale, A.M., Busa, E., Glessner, M., Salat, D., Hahn, H.K., Fischl, B., 2004. A hybrid approach to the skull stripping problem in MRI. NeuroImage 22 (3), 1060–1075.
Shalev-Shwartz, S., Ben-David, S., 2014. Understanding Machine Learning: From Theory to Algorithms. Cambridge university press.
Sheline, Y.I., Price, J.L., Yan, Z.Z., Mintun, M.A., 2010. Resting-state functional MRI in depression unmasks increased connectivity between networks via the dorsal nexus. Proc. Natl. Acad. Sci. U. S. A. 107 (24), 11020–11025. https://doi.org/10.1073/pnas.1000446107.
Skudlarski, P., Jagannathan, K., Anderson, K., Stevens, M.C., Calhoun, V.D., Skudlarska, B.A., Pearlson, G., 2010. Brain connectivity is not only lower but different in schizophrenia: a combined anatomical and functional approach. Biol. Psychiatry 68 (1), 61–69. https://doi.org/10.1016/j.biopsych.2010.03.035.
Sled, J.G., Zijdenbos, A.P., Evans, A.C., 1998. A nonparametric method for automatic correction of intensity nonuniformity in MRI data. IEEE Trans. Med. Imaging 17 (1), 87–97.
Sobell, L.C., Sobell, M.B., 2000. Alcohol Timeline Followback.
Spagnolli, F., Cerini, R., Cardobi, N., Barillari, M., Manganotti, P., Storti, S., Mucelli, R.P., 2013. Brain modifications after acute alcohol consumption analyzed by resting state fMRI. Magn. Reson. Imaging 31 (8), 1325–1330. https://doi.org/10.1016/j.mri.2013.04.007.
Squeglia, L.M., Ball, T.M., Jacobus, J., Brumback, T., McKenna, B.S., Nguyen-Louie, T.T., ... Tapert, S.F., 2017. Neural predictors of initiating alcohol use during adolescence. Am. J. Psychiatr. 174 (2), 172–185. https://doi.org/10.1176/appi.ajp.2016.15121587.
Sripada, C.S., Angstadt, M., McNamara, P., King, A.C., Phan, K.L., 2011. Effects of alcohol on brain responses to social signals of threat in humans. NeuroImage 55 (1), 371–380.
Steele, V.R., Claus, E.D., Aharoni, E., Vincent, G.M., Calhoun, V.D., Kiehl, K.A., 2015. Multimodal imaging measures predict rearrest. Front. Hum. Neurosci. 9, 425.
Steele, V.R., Maurer, J.M., Arbabshirani, M.R., Claus, E.D., Fink, B.C., Rao, V., ... Kiehl, K.A., 2018. Machine learning of functional magnetic resonance imaging network connectivity predicts substance abuse treatment completion. Biol. Psychiatry 3 (2), 141–149.
Stuke, H., Gutwinski, S., Wiers, C.E., Schmidt, T.T., Gropper, S., Parnack, J., ... Bermpohl, F., 2016. To drink or not to drink: harmful drinking is associated with hyperactivation of reward areas rather than hypoactivation of control areas in men. J. Psychiatry Neurosci. 41 (3), E24–E36. https://doi.org/10.1503/jpn.150203.
Sullivan, E.V., Pfefferbaum, A., 2005. Neurocircuitry in alcoholism: a substrate of disruption and repair. Psychopharmacology 180 (4), 583–594. https://doi.org/10.1007/s00213-005-2267-6.
Sussman, L., Grodin, E., Momenan, R., 2019. White matter microstructural differences between men and women with alcohol use disorder. Addict. Biol (Submitted).
Tagliazucchi, E., Laufs, H., 2014. Decoding wakefulness levels from typical fMRI resting-state data reveals reliable drifts between wakefulness and sleep. Neuron 82 (3), 695–708.
Takamura, T., Hanakawa, T., 2017. Clinical utility of resting-state functional connectivity magnetic resonance imaging for mood and cognitive disorders. J. Neural Transm. (Vienna) 124 (7), 821–839. https://doi.org/10.1007/s00702-017-1710-2.
Umut, G., Evren, C., Unal, G.T., 2017. Could childhood trauma types predict the relapse in alcohol use disorder? Asian J. Psychiatr. 25, 253. https://doi.org/10.1016/j.ajp.2016.12.009. Supplement C.
Van Dijk, K.R.A., Hedden, T., Venkataraman, A., Evans, K.C., Lazar, S.W., Buckner, R.L., 2010. Intrinsic functional connectivity as a tool for human connectomics: theory, properties, and optimization. J. Neurophysiol. 103 (1), 297–321. https://doi.org/10.1152/jn.00783.2009.
Varoquaux, G., 2018. Cross-validation failure: small sample sizes lead to large error bars. NeuroImage 180, 68–77. https://doi.org/10.1016/j.neuroimage.2017.06.061.
Vemuri, P., Wiste, H.J., Weigand, S.D., Shaw, L.M., Trojanowski, J.Q., Weiner, M.W., ... Alzheimers Dis Neuroimaging, I, 2009. MRI and CSF biomarkers in normal, MCI, and AD subjects predicting future clinical change. Neurology 73 (4), 294–301. https://doi.org/10.1212/WNL.0b013e3181af79fb.
Vengeliene, V., Bilbao, A., Molander, A., Spanagel, R., 2008. Neuropharmacology of alcohol addiction. Br. J. Pharmacol. 154 (2), 299–315. https://doi.org/10.1038/bjp.2008.30.
Vergara, V.M., Ulloa, A., Calhoun, V.D., Boutte, D., Chen, J., Liu, J., 2014. A three-way parallel ICA approach to analyze links among genetics, brain structure and brain function. NeuroImage 98, 386–394.
Vergara, V.M., Liu, J., Claus, E.D., Hutchison, K., Calhoun, V., 2017. Alterations of resting state functional network connectivity in the brain of nicotine and alcohol users. NeuroImage 151, 45–54. https://doi.org/10.1016/j.neuroimage.2016.11.012.
Vergara, V.M., Weiland, B.J., Hutchison, K.E., Calhoun, V.D., 2018. The impact of combinations of alcohol, nicotine, and cannabis on dynamic brain connectivity. Neuropsychopharmacology 43 (4), 877.
Wechsler, D., 2011. WASI-II: Wechsler Abbreviated Scale of Intelligence. Psychological Corporation.
Weiland, B.J., Sabbineni, A., Calhoun, V.D., Welsh, R.C., Bryan, A.D., Jung, R.E., ... Hutchison, K.E., 2014. Reduced left executive control network functional connectivity is associated with alcohol use disorders. Alcohol. Clin. Exp. Res. 38 (9), 2445–2453. https://doi.org/10.1111/acer.12505.
Wright, M.N., Ziegler, A., 2017. Ranger: a fast implementation of random forests for high dimensional data in C++ and R. J. Stat. Softw. 77, 1–17.
Yang, X., Tian, F., Zhang, H., Zeng, J., Chen, T., Wang, S., Gong, Q., 2016. Cortical and subcortical gray matter shrinkage in alcohol-use disorders: a voxel-based meta-analysis. Neurosci. Biobehav. Rev. 66, 92–103.
Yassa, M.A., Stark, S.M., Bakker, A., Albert, M.S., Gallagher, M., Stark, C.E.L., 2010. High-resolution structural and functional MRI of hippocampal CA3 and dentate gyrus in patients with amnestic Mild Cognitive Impairment. NeuroImage 51 (3), 1242–1252. https://doi.org/10.1016/j.neuroimage.2010.03.040.
Zhang, D.Q., Wang, Y.P., Zhou, L.P., Yuan, H., Shen, D.G., Alzheimers Dis Neuroimaging, I., 2011. Multimodal classification of Alzheimer's disease and mild cognitive impairment. NeuroImage 55 (3), 856–867. https://doi.org/10.1016/j.neuroimage.2011.01.008.
Zhou, Y., Liang, M., Tian, L.X., Wang, K., Hao, Y.H., Liu, H.H., Jiang, T.Z., 2007. Functional disintegration in paranoid schizophrenia using resting-state fMRI. Schizophr. Res. 97 (1–3), 194–205. https://doi.org/10.1016/j.schres.2007.05.029.
Zhu, X., Cortes, C.R., Mathur, K., Tomasi, D., Momenan, R., 2017. Model-free functional connectivity and impulsivity correlates of alcohol dependence: a resting-state study. Addict. Biol. 22 (1), 206–217. https://doi.org/10.1111/adb.12272.
Zhu, X., Du, X., Kerich, M., Lohoff, F.W., Momenan, R., 2018. Random Forest based classification of alcohol dependence patients and healthy controls using resting state MRI. Neurosci. Lett. 676, 27–33.
Zilverstand, A., Huang, A.S., Alia-Klein, N., Goldstein, R.Z., 2018. Neuroimaging impaired response inhibition and salience attribution in human drug addiction: a systematic review. Neuron 98 (5), 886–903.